Numerical Simulation and Control of Liquid Film Flow

MICHELLE C. VALLEJOS[1]
Department of Mathematics, University of the Philippines
Diliman, Quezon City, Philippines
e-mail: mcvallejos@up.edu.ph

and

RICARDO C.H. DEL ROSARIO[2]
Department of Mathematics, University of the Philippines
Diliman, Quezon City, Philippines
e-mail: rcdelros@math.upd.edu.ph

ABSTRACT

Kuramoto-Sivashinsky equation for long-wave motions of a thin film over a vertical plane is numerically discretized using the Galerkin method. We then employ feedback control methods in order to reduce the film fluctuation by blowing at different points on the wall surface. First, the control based on the linear system is used to control the flow, and then the control based on the nonlinear system is used. Numerical results show that the nonlinear control attenuates the system faster than the nonlinear one. For flows with high viscosity parameter, only one point actuator is needed to attain acceptable flow fluctuation attenuation, but for small viscosity parameter, two points are needed.

Keywords: Kuramoto-Sivashinsky equation, thin film flow, Linear Quadratic Regulator, Galerkin approximation.

1. Introduction

Liquid film flow on solid surfaces can be found both in nature and in industry. As early as the 1800s, various studies on the applications of liquid flows have been made. Liquid flow has continuously fascinated people due to the complexity of its properties. The fundamental description of liquid film flow is given by the Navier-Stokes equations. However, this system of four partial differential equations (PDEs), together with boundary conditions, seems to be very difficult to solve even for the most powerful modern computers [9]. It is fortunate that scientists were able to simplify the complex system without losing the most important features of its dynamic behavior. One such simplification, the Kuramoto-Sivashinsky (KS) equation, is one dimensional (with respect to the spatial variable) and hence theoretical analysis of the properties of its solution is much easier than with the full Navier-Stokes equations. It was first introduced by Kuramoto [11] in the study of phase turbulence in the Belousov-Zhabotinsky reaction. An extension to two or more spatial dimensions was then given by Sivashinsky [15] in the study of the propagation of flame front in the case of mild combustion. This equation

[1]M.C. Vallejos is a Ph.D. student in Mathematics at the University of Philippines
Email: mcvallejos@up.edu.ph

[2]R.C.H. del Rosario is an Associate Professor at the Department of Mathematics, University of the Philippines
Email: rcdelros@math.upd.edu.ph

has been widely used in different applications including concentration waves, plasma physics, flame propagation, reaction diffusion combustion dynamics, free surface film flows, and two-face flows in cylindrical or plane geometries [13]. Previous studies also include aspects of the statistical properties, the spectrum of Lyapunov exponents, the attractor/bifurcation map for small systems, and the stability analysis of the stationary solutions [5]. A favorable property of the KS equation is that it has self-sustained dynamics, i.e., it does not require external forcing (which would introduce additional parameters). The KS equation is also known to possess an attractor, which means that its long-time behavior is in fact finite-dimensional, the state dimension may nevertheless be still very high [14].

The goal of this study is to simulate liquid film flows using different viscosity parameters, and to implement feedback control methods in the simulations. We will consider the one-dimensional form of the KS equation which models the vertical motion of the liquid as it flows. The numerical method we will use is the Galerkin method using trigonometric functions as basis functions. This choice of basis functions comes from established results that the KS equation has trigonometric functions as modes (or eigenfunctions).

Our implementation of the Galerkin approximation method is straightforward. We did not exploit the existence of inertial manifolds as was done in [16] since we believe that the single KS equation in one spatial variable can be easily handled by a naive implementation of the Galerkin method. For problems with higher dimension, the exploitation of the peculiar properties of the system must be utilized in order to minimize computation time.

2. The Kuramoto-Sivashinsky Equation

Let $\eta(z,t)$ denote the distance of the film from the vertical plane (see Figure 1). The governing equation for the long-waves of the film are described by the Kuramoto-Sivashinsky equation [1, 2, 16] given by

$$\frac{\partial \eta}{\partial t} + \mu \frac{\partial^4 \eta}{\partial z^4} + \frac{\partial^2 \eta}{\partial z^2} + \eta \frac{\partial \eta}{\partial z} = 0 \tag{2.1}$$

where $z \in [-\pi, \pi]$, time $t \geq 0$, and $\mu > 0$ is the viscosity of the film. We denote the initial condition by

$$\eta(z,0) = \eta_0(z) \ ,$$

and we consider periodic boundary conditions given by

$$\frac{\partial^n}{\partial z^n}\eta(-\pi,t) = \frac{\partial^n}{\partial z^n}\eta(\pi,t) \ , \text{for } n = 0,1,2,3 \ .$$

Without loss of generality, we will restrict the domain on the interval $-\pi$ to π. This equation is valid only for strong surface-tension fluids where the wave height is smaller relative to its wavelength [1, 2].

3. The Numerical Method

In this section, we will describe the variational formulation of Equation (2.1) which is amenable to abstract analysis and numerical discretization methods.

In the derivation of the weak form of Equation (2.1), we will choose a test function $\phi(z)$ which satisfies the boundary conditions. Let the space of test functions be

$$V = \left\{ \phi \in C^\infty(-\pi,\pi) \middle| \frac{\partial^n}{\partial z^n}\phi(-\pi) = \frac{\partial^n}{\partial z^n}\phi(\pi) \ , \text{for } n = 0,1,2,3 \right\} \ ,$$

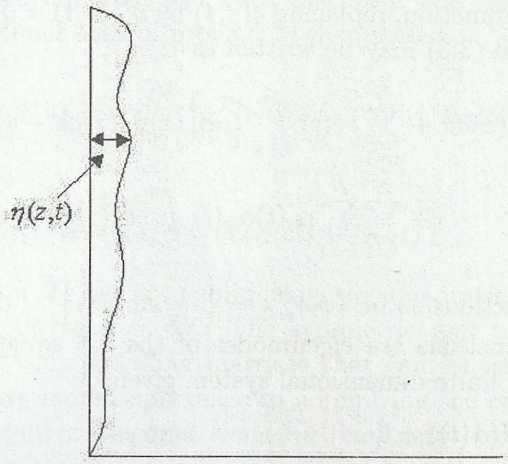

Figure 1: An illustration of the film flowing on a vertical plane.

where the space $C^\infty(-\pi,\pi)$ is the set of continuously differentiable functions defined on $(-\pi,\pi)$. Multiplying both sides of the KS equation by the test function $\phi(z)$ and then integrating over the domain, we obtain

$$\begin{aligned}\int_{-\pi}^{\pi}\frac{\partial\eta(z,t)}{\partial t}\phi(z)dz+\int_{-\pi}^{\pi}\mu\frac{\partial^4\eta(z,t)}{\partial z^4}\phi(z)dz+\int_{-\pi}^{\pi}\frac{\partial^2\eta(z,t)}{\partial z^2}\phi(z)dz\\+\int_{-\pi}^{\pi}\eta(z,t)\frac{\partial\eta(z,t)}{\partial z}\phi(z)dz=0\ .\end{aligned}\tag{3.2}$$

Using integration by parts on the second and third terms of Equation (3.2) and due to the boundary conditions we imposed on the test function ϕ, we can simplify the expression above in such a way that the weak form of Equation (2.1) is given by

$$\begin{aligned}\int_{-\pi}^{\pi}\frac{\partial\eta(z,t)}{\partial t}\phi(z)dz+\int_{-\pi}^{\pi}\mu\frac{\partial^2\eta(z,t)}{\partial z^2}\phi''(z)dz-\int_{-\pi}^{\pi}\frac{\partial\eta(z,t)}{\partial z}\phi'(z)dz\\+\int_{-\pi}^{\pi}\eta(z,t)\frac{\partial\eta(z,t)}{\partial z}\phi(z)dz=0\ ,\end{aligned}\tag{3.3}$$

wherein we want to find $\eta(\cdot,t)\in V$ for every $\phi\in V$. The main advantage of the weak form (3.3) over the strong form (2.1) is that in (3.3) we only need to differentiate twice in order to solve for η as opposed to (2.1) where we need to differentiate four times.

In the weak form (3.3), we seek the solution in the infinite dimensional space V for every test function ϕ. To solve the weak form numerically, we will solve the weak form in a finite-dimensional subspace of V. Consider an N-dimensional subspace of V with basis $\phi_1,\phi_2,\ldots,\phi_N$, i.e.,

$$V^N=\text{span}\,\{\phi_1,\phi_2,\ldots,\phi_N\}\subset V\ .$$

Since we seek the solution in V^N, the finite-dimensional solution can be written in the form

$$\eta^N(z,t)=\sum_{i=1}^{N}\alpha_i(t)\phi_i(z)\ .$$

The finite-dimensional analog of the weak form is therefore given by: find $\eta^N(\cdot,t)\in V^N$ such that η^N satisfies (3.3) for all $\phi\in\{\phi_1,\phi_2,\ldots,\phi_N\}$.

Using $\phi_j(z)$ as the test function, replacing $\eta(z,t)$ by $\eta^N(z,t) = \sum_{i=1}^N \alpha_i(t)\phi_i(z)$, and using the notation $\frac{\partial z}{\partial t} = \dot{z}$, Equation (3.3) may be written as

$$\sum_{i=1}^N \dot{\alpha}_i(t) \int_{-\pi}^{\pi} \phi_i(z)\phi_j(z)dz + \sum_{i=1}^N \alpha_i(t) \int_{-\pi}^{\pi} \left[\mu\phi_i''(z)\phi_j''(z)dz - \phi_i'(z)\phi_j'(z)\right] dz + \sum_{i=1}^N \sum_{k=1}^N \alpha_i(t)\alpha_k(t) \int_{-\pi}^{\pi} \phi_i(z)\phi_k'(z)\phi_j(z) = 0 \ .$$

We chose the basis functions to be $\{\phi_i\}_{i=1}^N = \left\{\frac{1}{\sqrt{\pi}} \sin(iz)\right\}_{i=1}^N$ due to theoretical results that indicate that the sine functions are eigenmodes of the KS equation. Galerkin discretization yields the (semi-discrete) finite dimensional system given by

$$\begin{aligned} &M\dot{\alpha}(t) + A\alpha(t) + N(\alpha(t)) = 0 \\ &\alpha(0) = \alpha_0 \ , \end{aligned} \tag{3.4}$$

where the matrices are as follows

$$[M]_{j,i} = \int_{-\pi}^{\pi} \phi_i(z)\phi_j(z)dz \ , \quad [A]_{j,i} = \int_{-\pi}^{\pi} \left\{\mu\phi_i''(z)\phi_j''(z) - \phi_i'(z)\phi_j'(z)\right\} dz \ ,$$

$$N(\alpha(t)) = \begin{bmatrix} \alpha^T(t)K_1\alpha(t) \\ \vdots \\ \alpha^T(t)K_N\alpha(t) \end{bmatrix} \ , \quad [K_j]_{k,i} = \int_{-\pi}^{\pi} \phi_i(z)\phi_k'(z)\phi_j(z)dz \ ,$$

$$\alpha(t) = \begin{bmatrix} \alpha_1(t) \\ \vdots \\ \alpha_N(t) \end{bmatrix} \text{ and } \qquad \eta_0(z) = \sum_{i=1}^N \alpha_0\phi_i(z) \ .$$

Note that (3.4) is a system of N first-order nonlinear ODEs. Numerical methods must be used to solve the system from the starting time $t = 0$ up to an ending time. We will use readily available numerical ODE solvers such as the explicit Runge-Kutta solvers of order four with variable step sizes.

4. The Control Method

Feedback control methods are implemented to reduce the film fluctuation by blowing or suctioning at different points on the wall surface. In order to reduce the fluctuation of the flow (i.e., the distance of the liquid from the wall surface), we will model point actuators at different locations on the wall surface. Air can be either blown or sucked at these points. Suppose we have M_c actuators located at $z_1, z_2, \ldots, z_{M_c}$ (all within the interval $[-\pi, \pi]$). Then an external (point) force acting on the film is introduced at these points and the KS equation is now of the form

$$\frac{\partial\eta}{\partial t} + \mu\frac{\partial^4\eta}{\partial z^4} + \frac{\partial^2\eta}{\partial z^2} + \eta\frac{\partial\eta}{\partial z} = F_c(z,t) \ , \tag{4.5}$$

where the force term $F_c(z,t)$, on the right hand side is given by

$$F_c(z,t) = \sum_{i=1}^{M_c} u_i(t)\delta(z - z_i) \ .$$

The magnitude of blowing or suctioning at z_i is given by $u_i(t)$ and the Dirac delta function $\delta(z - z_i)$ assures that the control $u_i(t)$ is active only at the point z_i. A Linear Quadratic

Regulator (LQR) Problem is formulated, and both the linear and nonlinear feedback control gains were computed. The optimal control problem is then stated as

$$\text{minimize } J(u) = \frac{1}{2}\int_0^\infty \left[\alpha^T(t)Q\alpha(t) + u^T(t)Ru(t)\right] dt$$

subject to

$$\dot{\alpha}(t) = -A\alpha(t) - N(\alpha(t)) + Bu(t) \ .$$

Note that in the cost function J, we are minimizing the quadratic terms $\alpha^T(t)Q\alpha(t)$ and $u^T(t)Ru(t)$ from time $t = 0$ up to $t = \infty$. The symmetric and positive-definite matrices $Q \in \mathbb{R}^{N\times N}$ and $R \in \mathbb{R}^{M_c\times M_c}$ are weighing matrices that can be used to give more importance to minimizing α or to give more importance to minimizing the control u. These matrices are usually chosen to have positive diagonal elements (and zero elsewhere). Hence, the i^{th} diagonal element of Q, say q_i, places a q_i weight to the i^{th} component of the vector $\alpha(t)$.

4.1. Linear Feedback Control

Let us first assume that the nonlinear part $N(\alpha(t))$ is very small such that it hardly affects the system. This assumption is analogous to the dropping of the nonlinear term in the Navier-Stokes equations which yields the linear stokes equation. The optimal control problem is now given by

$$\text{minimize } J(u) = \frac{1}{2}\int_0^\infty \left[\alpha^T(t)Q\alpha(t) + u^T(t)Ru(t)\right] dt$$

subject to

$$\dot{\alpha}(t) = -A\alpha(t) + Bu(t) \ .$$

The optimal control based on the linear system is given by

$$u^*(t) = -R^{-1}B^T\Pi\alpha(t) \ ,$$

where Π is the solution to the Algebraic Riccati Equation

$$\Pi A + A^T\Pi - \Pi BR^{-1}B^T\Pi + Q = 0 \ .$$

The optimal control u^* is in feedback form, i.e., the current state $\alpha(t)$ is used to solve for the optimal control at time t. For this linear based control, we obtain the closed loop system

$$\dot{\alpha}(t) = -(A + BR^{-1}B^T\Pi)\alpha(t) \ .$$

4.2. Nonlinear Feedback Control

Similar arguments used in computing the optimal control for the linear case can be used for the nonlinear dynamical system. Thus, the nonlinear feedback control $u^*(t)$ is given by

$$u^*(t) = -R^{-1}B^T[\Pi\alpha(t) - (A^T - \Pi BR^{-1}B^T)^{-1}\Pi N(\alpha(t))],$$

and in this case, the closed loop is

$$\dot{\alpha}(t) = -\left(A + BR^{-1}B^T\Pi\right)\alpha(t) - \left[I - BR^{-1}B^T(A^T - \Pi BR^{-1}B^T)^{-1}\Pi\right]N(\alpha(t) \ .$$

5. Numerical Results

In our numerical computations, we will use $N = 5$ basis functions, namely

$$\begin{aligned} \phi_1(z) &= \tfrac{1}{\sqrt{\pi}} sin(z), \qquad \phi_3(z) = \tfrac{1}{\sqrt{\pi}} sin(3z), \text{ and } \quad \phi_5(z) = \tfrac{1}{\sqrt{\pi}} sin(5z). \\ \phi_2(z) &= \tfrac{1}{\sqrt{\pi}} sin(2z), \qquad \phi_4(z) = \tfrac{1}{\sqrt{\pi}} sin(4z), \end{aligned} \tag{5.6}$$

We will simulate the uncontrolled system using the following values for the viscosity: $\mu = 0.3$, $\mu = 0.5$ and $\mu = 0.15$, corresponding respectively to "semi"-viscous, viscous and "less" viscous flow. We will also consider different initial conditions. These initial conditions are specified by choosing the coefficients of the basis functions in expressing the initial state as a linear combination of $\phi_1, \phi_2, \ldots, \phi_5$, i.e., $\eta^N(z,0) = \eta_0^N(z) = \sum_{i=1}^{5} \alpha_i \phi_i(z)$. We will simply denote the vector of initial conditions $[\alpha_1, \alpha_2, \ldots, \alpha_5]^T$ by α_0.

In our implementation of LQR control, the matrices Q and R were chosen to be the identity matrices of sizes $N \times N$ and $M_c \times M_c$, respectively. We will get ahead of ourselves by saying that these identity weighing matrices already produced acceptable attenuation of the film fluctuations, hence other values for Q and R were not considered anymore. We would like to point out that bigger values for Q such as $Q = 100 I^{N \times N}$ should theoretically produce better attenuation but the control results we obtain did not exhibit significant improvement.

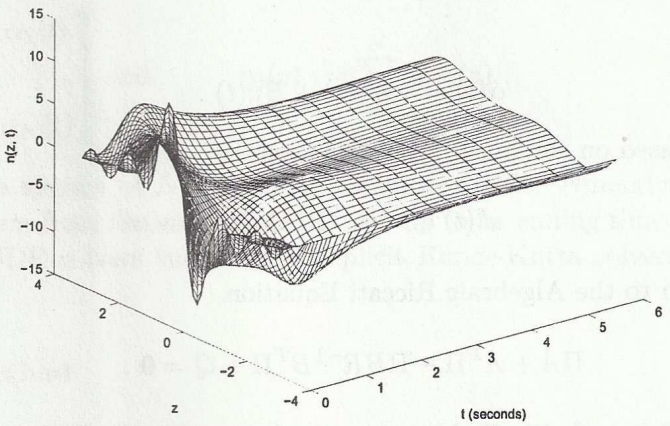

Figure 2: Uncontrolled simulation with $\mu = 0.3$ and $\alpha_0 = [5\ 5\ 5\ 5\ 5]^T$.

Let us first consider the initial condition $\alpha_0 = [5\ 5\ 5\ 5\ 5]^T$. The uncontrolled simulation with $\mu = 0.3$ from $t = 0$ up to $t = 6$ is shown in Figure 2. The controlled system (with $\mu = 0.3$) using control based on the linear model is shown in Figure 3 and the controlled system using control based on nonlinear model is shown in Figure 4. It can be seen in Figures 2 to 4 that the controlled simulations exhibit less fluctuations than in the uncontrolled case and that the control based on the nonlinear model attenuates the fluctuations faster than the linear based control. To illustrate this better, we plot in Figure 5 the film fluctuation η at $z = \frac{\pi}{2}$ for the uncontrolled, linear controlled and nonlinear controlled simulations. It can be seen in Figure 5 that the nonlinear control does indeed minimize the fluctuations faster than linear control. Note that Figure 5 is the cross section at $z = \frac{\pi}{2}$, where the actuator is actually located. Hence we expect the control to perform well here.

To anwser the question on how our control method affects points away from the actuator, we also plot the cross section at $z = \pi$ in Figure 6 and note that a similar behavior of the control is exhibited as in Figure 5. To illustrate the magnitude of the blowing or suctioning used to control the flow, we plot the optimal control $u(t)$ using linear and nonlinear computations in Figure 7. Figure 7 assures that the magnitude of blowing or suctioning is limited to a certain range, and it even goes to zero as $t \to \infty$.

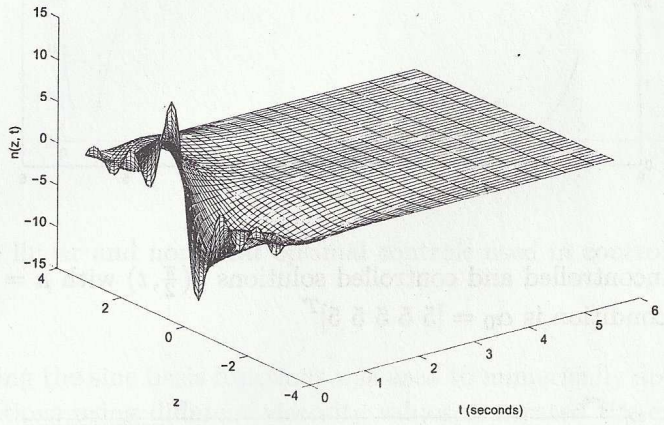

Figure 3: Simulation using linear control with $\mu = 0.3$ and an actuator at $z = \frac{\pi}{2}$. The initial condition is $\alpha_0 = [5\ 5\ 5\ 5\ 5]^T$.

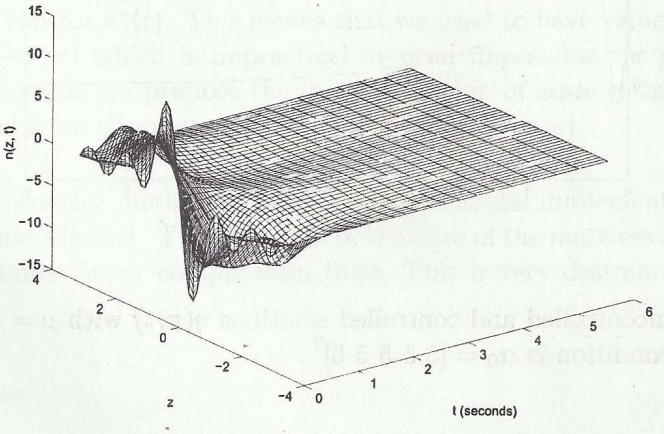

Figure 4: Simulation using nonlinear control with $\mu = 0.3$ and an actuator at $z = \frac{\pi}{2}$. The initial condition is $\alpha_0 = [5\ 5\ 5\ 5\ 5]^T$.

We will now illustrate that the method can handle different viscosities. We will now use a more"wavy" initial condition $\alpha_0 = [5\ 3\ 1\ 3\ 5]^T$, and plot control results for $\mu = 0.3$, $\mu = 0.5$, and $\mu = 0.15$ in Figures 8, 9 and 10 respectively. In each figure, the uncontrolled, linear controlled, and the nonlinear controlled simulations are presented, together with a cross section at $z = \frac{\pi}{2}$.

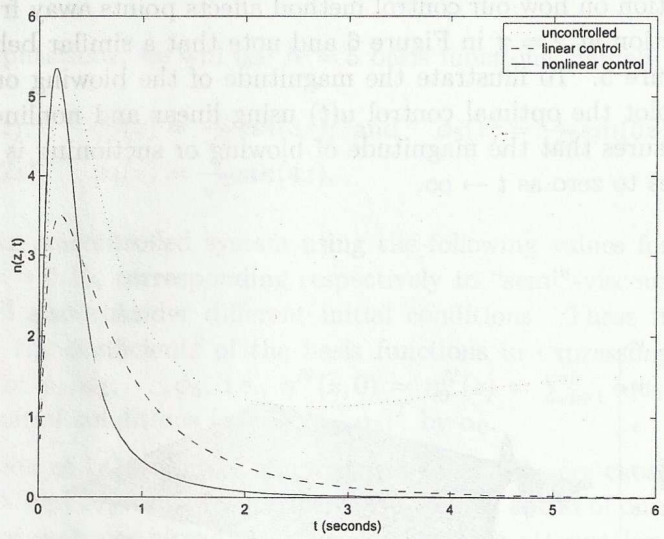

Figure 5: Plot of the uncontrolled and controlled solutions $\eta(\frac{\pi}{2}, t)$ with $\mu = 0.3$ and an actuator at $z = \frac{\pi}{2}$. The initial condition is $\alpha_0 = [5\ 5\ 5\ 5\ 5]^T$.

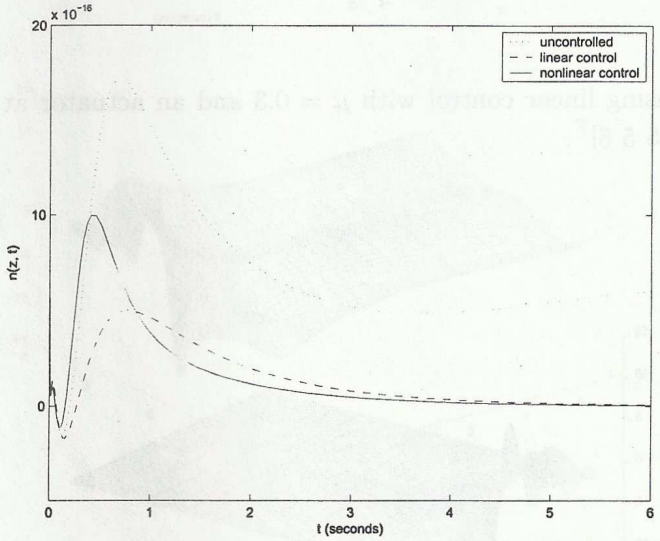

Figure 6: Plot of the uncontrolled and controlled solutions $\eta(\pi, t)$ with $\mu = 0.3$ and an actuator at $z = \frac{\pi}{2}$. The initial condition is $\alpha_0 = [5\ 5\ 5\ 5\ 5]^T$.

We needed to use two point actuators for the less viscous flow, $\mu = 0.15$, located at $z = \frac{\pi}{3}$ and $z = \frac{2\pi}{3}$, as opposed to one point actuator at $z = \frac{\pi}{2}$ for $\mu = 0.3$ and $\mu = 0.5$. This is expected since it is more difficult to control less viscous flow.

6. Conclusions

In this paper, we have illustrated the use of optimal control methods in minimizing the fluctuations of thin film flow. The Kuramoto-Sivashinsky equation was used to model the system and a

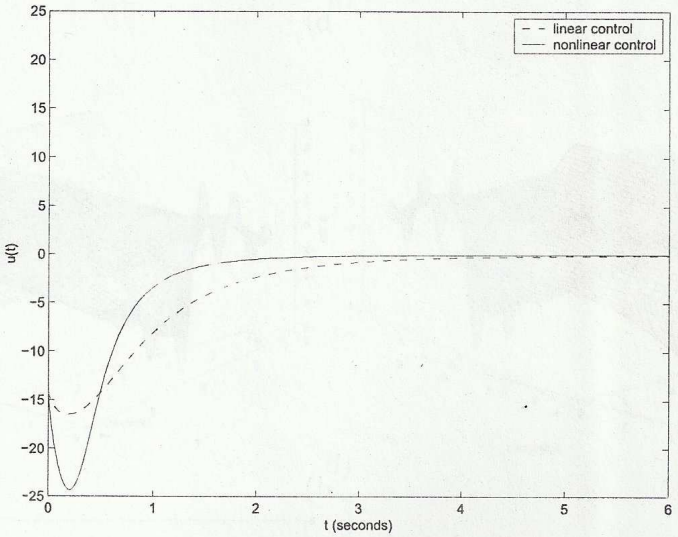

Figure 7: Plot of the linear and nonlinear optimal controls used in controlling Figures 3 and 4, respectively.

Galerkin method using the sine basis functions was used to numerically approximate the system. Uncontrolled simulations using different viscosity values illustrated the expected behavior that the viscosity of the liquid is directly (positively) related to the stability of the waves. Viscous fluids exhibit less fluctuations than the less viscous one. For less viscous flow, two controllers were needed to minimize fluctuations. We were able to show that both linear model-based control and nonlinear model-based control minimizes film fluctuations (using different viscosities and initial conditions). Furthermore, we were also able to exhibit the expected result that the nonlinear based control attenuates film fluctuation faster than the linear based control.

The control method we implemented assures that the full state at time t is available for computing the feedback control $u^*(t)$. This means that we need to have values for the displacement η at all points in $(-\pi, \pi)$ which is impractical or even impossible for practical applications. Therefore, for future work, we propose the implementation of state estimators so that the full state is reconstructed from observations at a few points in $(-\pi, \pi)$.

Furthermore, to make this method more applicable to actual implementation, basis reduction methods should be investigated. The reduction of the sizes of the matrices arising from numerical methods will allow much faster computation time. This is very desirable for real-time control implementation.

Acknowledgements

The authors would like to thank Dr. H. T. Tran of North Carolina State University for giving this topic, and also HRDO and the Heuristics Group for the thesis funding.

References

[1] D.J. Benny, Long Waves in Liquid Films. *Journal of Mathematical Physics* **45** (1966), 150–155.

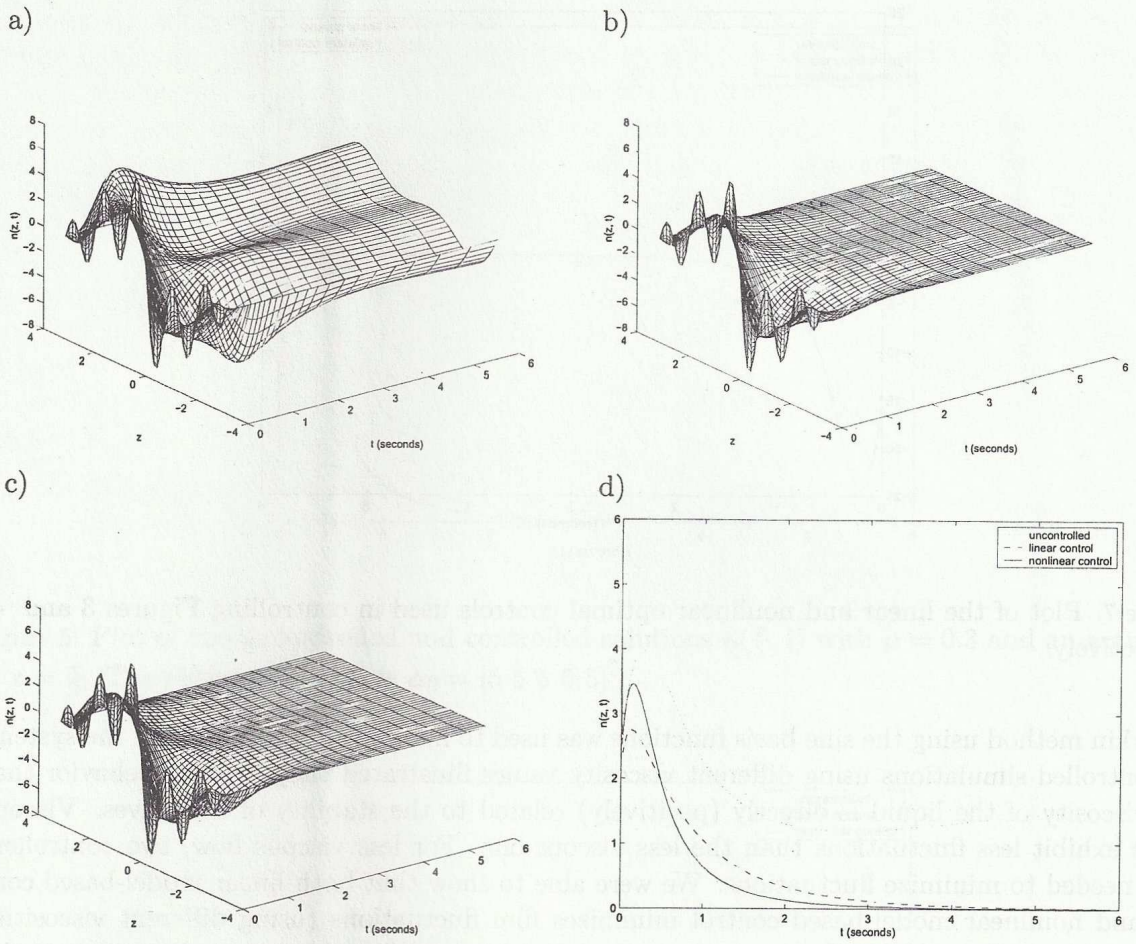

Figure 8: a) Uncontrolled simulation with $\mu = 0.3$ and $\alpha_0 = [5\ 3\ 1\ 3\ 5]^T$. b) Simulation using linear control with an actuator at $z = \frac{\pi}{2}$. c) Simulation using nonlinear control with an actuator at $z = \frac{\pi}{2}$. d) Plot of the uncontrolled and controlled solutions $\eta(\frac{\pi}{2}, t)$ with an actuator at $z = \frac{\pi}{2}$.

[2] C.H. CHANG, Wave Evolution on a Falling Film. *Journal of Mathematical Physics* **26** (1994), 103–136.

[3] G. CHEN, C. LI, Bifurcation Analysis of the Kuramoto Sivashinsky Equation in One Spatial Dimension. *International Journal of Bifurcation and Chaos* **9** (2001), 2493–2499.

[4] G. CHEN, C. LI, Bifurcation from an Equilibrium of the Steady State Kuramoto Sivashinsky Equation in Two Spatial Dimensions. *International Journal of Bifurcation and Chaos* **12** (2002), 103–114.

[5] C. CHOW, T. HWA,, Defect-Mediated Stability: An Effective Hydrodynamic Theory of Spatiotemporal Chaos. *Physica D* **84** (1995), 494–512.

[6] F. CSAKI, Modern Control Theories: Nonlinear, Optimal and Adaptive Systems. Akademiai Kiado, Budapest, (1972)

[7] R.C.H. DEL ROSARIO, *Computational Methods for Feedback Control in Structural Systems.* N. C. State University, (1998).

[8] W. FLEMING, R. RISHEL, *Deterministic and Stochastic Optimal Control.* New York: Springer-Verlag,(1975).

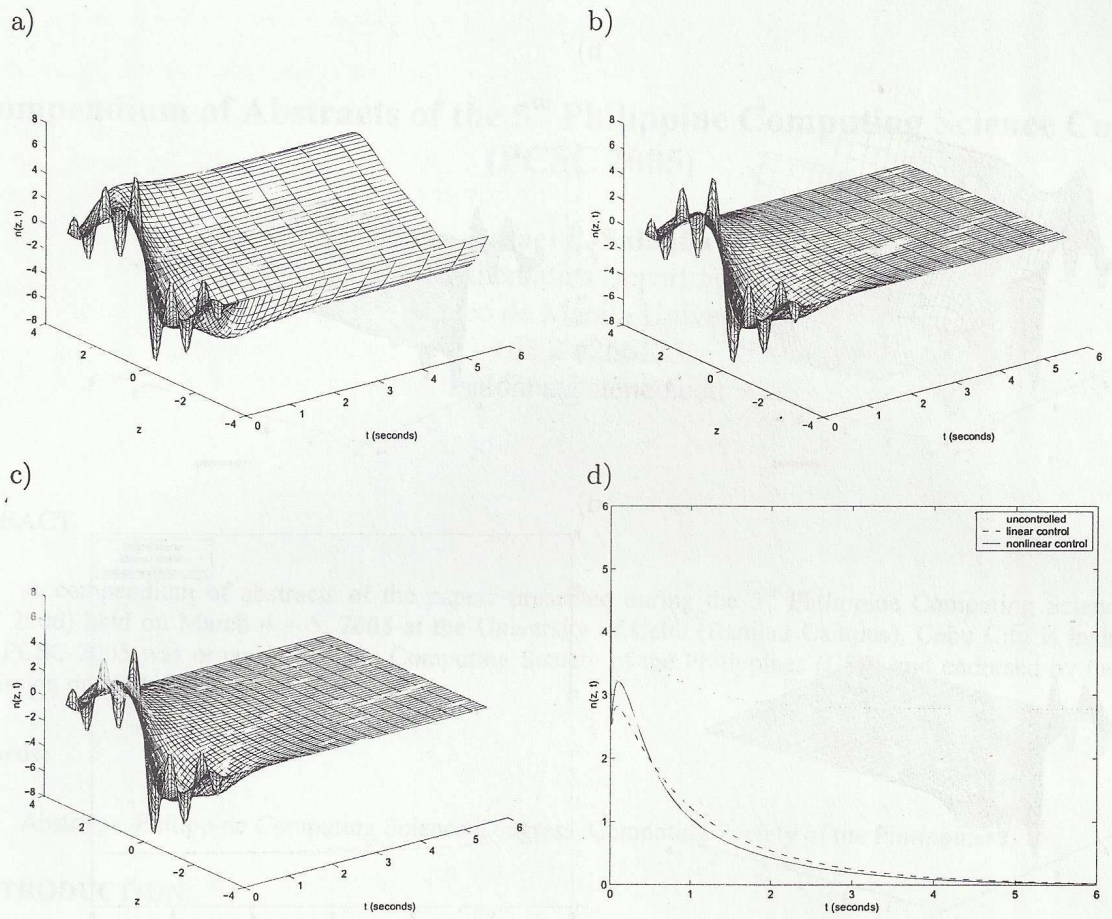

Figure 9: a) Uncontrolled simulation with $\mu = 0.5$ and $\alpha_0 = [5\ 3\ 1\ 3\ 5]^T$. b) Simulation using linear control with an actuator at $z = \frac{\pi}{2}$. c) Simulation using nonlinear control with an actuator at $z = \frac{\pi}{2}$. d) Plot of the uncontrolled and controlled solutions $\eta(\frac{\pi}{2}, t)$ with an actuator at $z = \frac{\pi}{2}$.

[9] A. Frenkel, K. Indireshkumar, Spatiotemporal Patterns in a 3-D Film Flow.*Proceedings of the AMS-IMS-SIAM Summer Research Conference, Seattle; ed. Y. Renardy et al.* Philadelphia, (1995), 288–309.

[10] D. Jacobs, *Introduction to Control Theory.* Oxford: Clarendon Press,(1974).

[11] Y. Kuramoto, *Diffusion Induced Chaos in Reaction Systems.* Prog. Theoret. Phys. Suppl., (1978).

[12] B. Nicolaenko, J. Hyman, *The Kuramoto-Sivashinsky Equation: A Bridge Between PDE's and Dynamical Systems.* Physica 18D, (1986), 113–126.

[13] D. Papageorgiou, Computational Study of Chaotic and Ordered Solutions of the Kuramoto-Sivashisky Equation. *NASA CR-198283 ICASE Report No. 96-12,* Institute for Computer Applications in Science and Engineering Mail Stop 132C, NASA Langley Research Center, Hampton, (1996).

[14] B. Protas, *Some Formulation Issues in Adjoint-Based Optimal Estimation and Control of PDEs. Case Study of the Kuramoto-Sivashinsky Equation,* (1995).

[15] G. Sivashinsky, D. Michelson, Nonlinear Analysis of Hydrodynamics Instability in Laminar Flames. *Acta Astronautica* Vol. 4, (1977), 1207–1221.

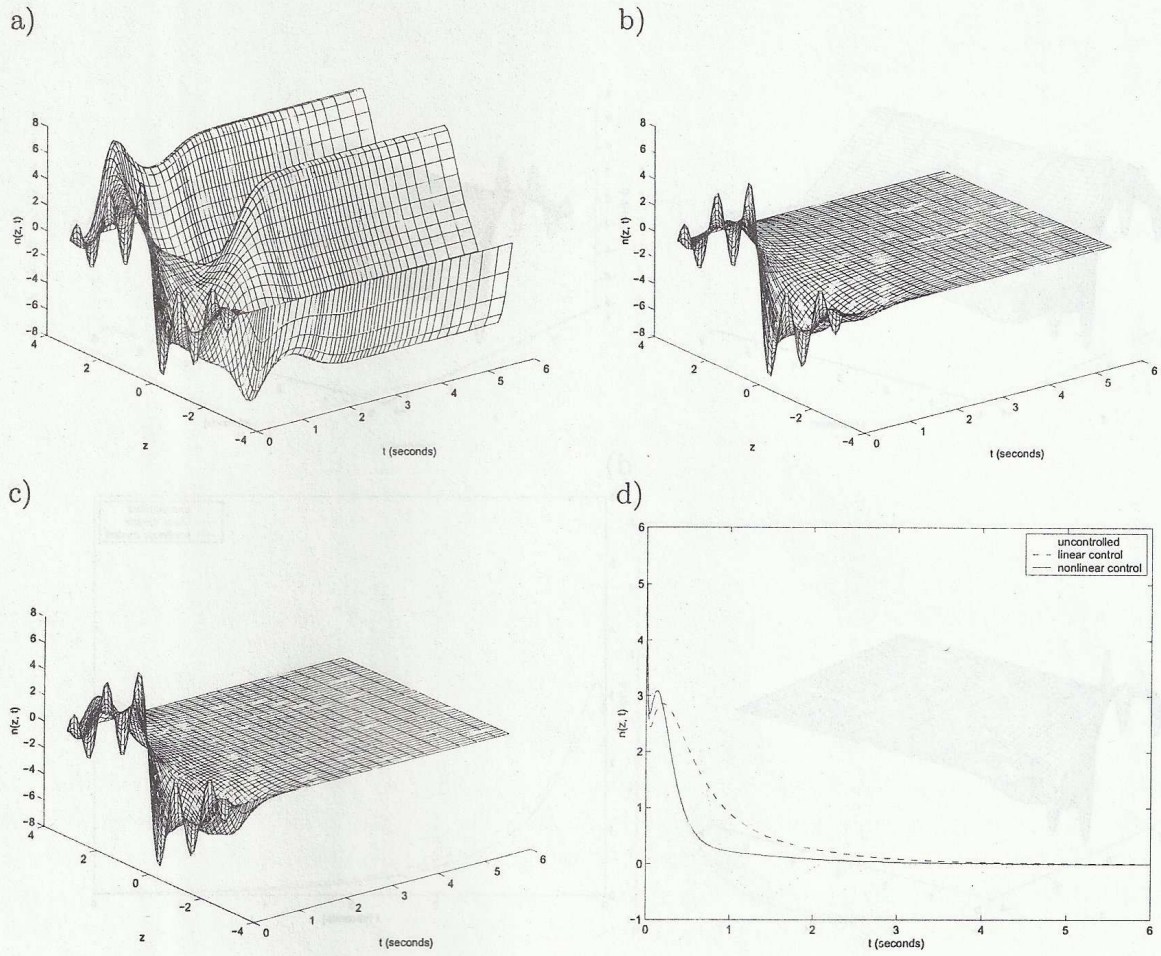

Figure 10: a) Uncontrolled simulation with $\mu = 0.15$ and $\alpha_0 = [5\ 3\ 1\ 3\ 5]^T$. b) Simulation using linear control with two actuators at $z = \frac{\pi}{3}$ and $z = \frac{2\pi}{3}$. c) Simulation using nonlinear control with two actuators at $z = \frac{\pi}{3}$ and $z = \frac{2\pi}{3}$. d) Plot of the uncontrolled and controlled solutions $\eta(\frac{\pi}{2}, t)$ with two actuators at $z = \frac{\pi}{3}$ and $z = \frac{2\pi}{3}$.

[16] H. Tran, C. Lee, *Reduced-Order Feedback Control for Liquid Film Flows. Journal of Computational and Applied Mathematics*, (2000).